

# Behavior of mine tailings under cyclic hydraulic loading

Africa M. Geremew and Ernest K. Yanful

**Abstract:** Shallow water cover is one of the most effective methods of managing sulfide-bearing reactive mine tailings. Unless sufficient water cover depth is provided, surface erosion by wind-induced waves and pressure-driven currents can re-suspend the tailings and expose them to dissolved oxygen and affect the quality of the water cover. The present study gives a simple approach for the estimation of the critical shear stress for surface erosion of mine tailings and cohesive sediments under shallow water cover. Erosion tests were carried out in a Plexiglas laboratory annular column on mine tailings and sediments under a 50 cm water cover. The annular column was 30 cm in diameter, 120 cm in height and had a 9 cm annular flow width. Shear stress was introduced through a motor driven Teflon stirrer to investigate the initiation of motion and subsequent re-suspension of newly deposited mine tailings and sediments. The velocity field and the pressure change in the boundary layer were measured by laser Doppler velocimeter (LDV) and Preston tube, respectively. The ranges of critical shear stress for the tailings and sediments were estimated by the LDV and Preston tube measurements and visual observation. The results showed that the erosion behavior of most of the mine tailings can be explained by a power law erosion equation.

*Key words:* cohesive sediments, Preston tube, LDV, critical shear stress, erosion rate.

**Résumé :** Une couverture aquatique peu profonde est l'une des méthodes les plus efficaces de gestion des résidus miniers contenant des sulfures réactifs. Si la couverture aquatique n'est pas suffisamment profonde, une érosion de surface par des vagues générées par le vent et des courants générés par la pression du vent pourraient remettre en suspension les résidus et les exposer à l'oxygène dissous, affectant ainsi la qualité de la couverture aquatique. La présente étude traite d'une approche simple d'estimation de la contrainte de cisaillement critique pour l'érosion de surface des résidus miniers et des sédiments cohésifs sous une mince couverture aquatique. Des essais d'érosion ont été réalisés dans une colonne annulaire en Plexiglas en laboratoire sur les résidus miniers et des sédiments sous une couverture aquatique de 50 cm. La colonne annulaire mesure 30 cm de diamètre, 120 cm de hauteur et a un écoulement annulaire de 9 cm. La contrainte de cisaillement était générée par un agitateur en Teflon actionné par moteur pour étudier l'amorçage du mouvement et de la remise en suspension subséquente des résidus miniers et des sédiments nouvellement déposés. Le champ de vitesse et le changement de pression dans la couche limite ont été mesurés respectivement au moyen d'un vélocimètre Doppler à laser et d'un tube de Preston. Les plages de contraintes de cisaillement critique ont été estimées pour les résidus miniers et les sédiments au moyen de mesures par vélocimètre Doppler à laser, par un tube de Preston et par des observations visuelles. Les résultats montrent que le comportement à l'érosion de la majorité des résidus miniers peut être expliqué par une équation d'érosion à une puissance donnée.

*Mots-clés :* sédiments cohésifs, tube de Preston, vélocimètre Doppler à laser, contrainte de cisaillement critique, taux d'érosion.

[Traduit par la Rédaction]

## Introduction

A vast amount of fine-grained milling wastes and tailings are produced in mineral processing plants each day. Effective and economical disposal of these wastes in an environmentally friendly manner has become a major issue facing

mining operations. The use of a shallow water cover is one of the most effective methods of managing unoxidized sulfidic mine tailings (Robertson et al. 1997). This is due to the fact that the rate of oxygen diffusivity and solubility in water is dramatically lower than in air. However, the re-suspension of flooded mine wastes may threaten the effectiveness of a water cover.

Mine tailings ponds are usually designed taking into account the hydrologic water balance, effect of wind-induced shear stress at the tailings bed surface, bed shear stress due to return currents and erosion resistance of the tailings. It has been shown in specific site studies that mine tailings predominantly exhibit cohesive behavior and their erosion behavior is different from non-cohesive sediments (Mian and Yanful 2007). One of the main challenges in water cover design is the prediction of mine tailings erosion behavior and their subsequent re-suspension as the physics of

Received 12 January 2010. Revision accepted 18 November 2010. Published on the NRC Research Press Web site at [cjce.nrc.ca](http://cjce.nrc.ca) on 17 December 2010.

**A.M. Geremew<sup>1</sup> and E.K. Yanful.** Department of Civil and Environmental Engineering, The University of Western Ontario, 1151 Richmond Street North, London, ON N6A 5B9, Canada.

Written discussion of this article is welcomed and will be received by the Editor until 30 June 2011.

<sup>1</sup>Corresponding author (e-mail: [ageremew@uwo.ca](mailto:ageremew@uwo.ca)).

mine tailings erosion is not well established. Therefore, the main objective of this study was to establish an improved and simplified method to investigate mine tailings erosion behaviour and to estimate the critical shear stress for erosion and the erosion rate of mine tailings.

The difference between the current study and the previous work by Mian et al. (2007) includes the following: (1) The current study uses an annular column that reduces the vorticity created with the Teflon stirrer by re-routing and channeling the flow in an annular manner. Mian et al. (2007) used a single open cylindrical column which tends to generate significant vorticity in the flow. (2) The current study uses the Preston tube to estimate the bed shear stress in addition to laser Doppler velocimetry (LDV) measurements whereas Mian et al. (2007) used LDV alone. The Preston tube method is simpler, economical and the device is portable so that it can also be used in the field to estimate critical shear stress. (3) In the present study the critical shear stress was also determined from visual observations and examinations during the erosion experiment. This is not included in the study by Mian et al. (2007).

## Materials and methods

### Samples description

The samples used in this study were Shebandowan-I, Shebandowan west cell, Mattabi, Musselwhite, Musselwhite – 5% kaolinite, Musselwhite – 15% kaolinite, and Musselwhite – 5% bentonite tailings, Casco clayey silt and London sand. Unoxidized mine tailings were obtained from Shebandowan-I and Shebandowan west cell tailings pond located near Shebandowan Lake approximately 90 km west of Thunder Bay, Ontario, Canada. Mine tailings were obtained from Mattabi mine tailings site near Ignace, Ontario, Canada. Mine tailings were also obtained from Musselwhite mine located 480 km north of Thunder Bay, Ontario. The other mine tailings were obtained from Sudbury copper cliff mines at Sudbury, located about 400 km north of Toronto, Ontario. Kaolinite and Wyoming bentonite obtained from the USA were also used in the study. The other two samples, Casco clayey silt and London sand, which did not contain sulfide-bearing minerals, were used for comparison purposes.

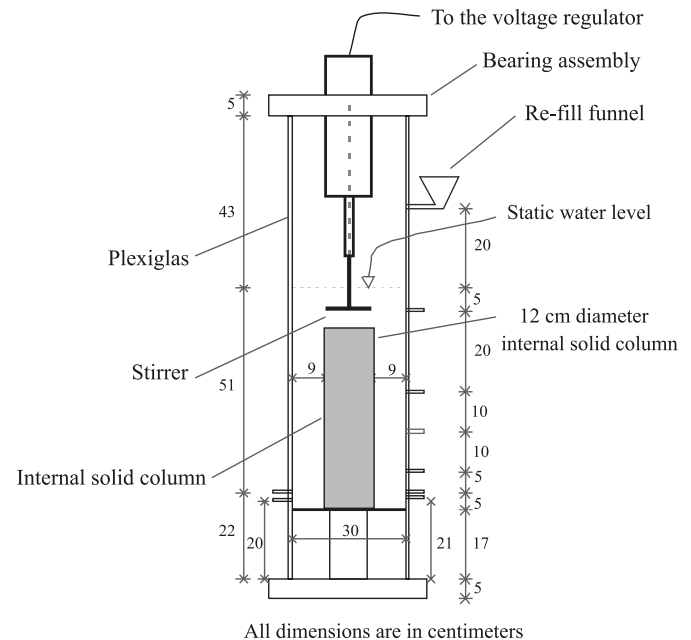
### Characterization of tailings and sediments for basic physical properties

In the present study, a series of laboratory tests were carried out using standard testing methods to obtain the basic physical properties of the tailings and the sediments. The particle size distribution of the tailings and the sediments were obtained using the standard sieve and hydrometer analysis (ASTM 152-H). Specific gravity and Atterberg limits tests were also measured using ASTM D-4318. The tailings and the sediments were classified using the Unified Classification System based on ASTM D-2487 (Braja 2002).

### Laboratory annular column description

The erosion experiments were performed in a transparent circular laboratory Plexiglas annular column with an internal diameter of 30 cm, a height of 1.25 m, and a thickness of 1 cm. The annular flow width of the column was 9 cm. A

**Fig. 1.** The experimental (laboratory) annular column.



3 cm thick PVC (polyvinyl chloride) plate was screwed to its bottom with a connection gasket to ensure water-tightness. A 1 cm thick circular plate, made of Plexiglas, with a radius of 30 cm was fixed at 17 cm above the bottom of the column. This intermediate circular plate was supported by wooden pillars and was well glued with the wall of the column to ensure water-tightness. The column had nine 1 cm diameter openings on its wall. Four of the openings, located at 10, 20, 30 and 50 cm from the surface of the intermediate plate, were used as sampling ports. One opening, located at 75 cm from the surface of the intermediate plate, was used for adding water to replace the small volume of suspension taken for the measurement of suspended solids concentration. The other two, located at 5 cm from the intermediate plate were for total and static pressure measurement. The remaining two openings, located at 3 and 4 cm above the surface of the intermediate plate, were for pore water pressure measurements. A 50 cm long two-blade Teflon stirrer was used to introduce bed shear stress. Each blade of the Teflon stirrer was 6 cm in length and 1 cm in thickness. As shown in Fig. 1, the top 3 cm PVC cover plate of the column was fitted with a bearing assembly to ensure that the stirrer was stationary. The stirrer was controlled by an alternating current (AC) motor and the input power to the stirrer was regulated by a direct current (DC) voltage regulator; the stirrer speed was calibrated against the voltage regulator with an accuracy of  $\pm 2\%$ .

In an open column without a solid central core, vorticity is generated at 5 cm below the water level (i.e., 45 cm above the tailings or sediments surface) in the middle portion of the column where the stirrer blade is located. The generated vorticity can significantly affect the flow field in the column and travel down to the surface of the deposited tailings or sediments bed, depending on the applied stirrer speed. This flow field could lead to the accumulation of tailings or sediments at the centre of the column and can reduce the accuracy of the estimated critical bed shear stress and



sampling, an equivalent volume of water was re-filled through the re-filling funnel (Fig. 1). The concentration of suspended solids for each stirrer speed was estimated by oven drying the corresponding sampled suspension at 100 °C for approximately 24 h. By doing so, the average concentration of re-suspended materials was related to the stirrer speed of the motor which, in turn, was related to the bed shear stress.

## Results and discussion

### Basic physical properties of the tailings and sediments

The basic physical properties of Shebandowan-I, Shebandowan west cell, Mattabi, Musselwhite, Musselwhite – 5% kaolinite, Musselwhite – 15% kaolinite, and Sudbury tailings, and London sand and Casco clayey silt obtained from laboratory tests are presented in Table 1. As expected, the grain size distributions of the tailings fall between those of Casco clayey silt and London sand. As shown in Table 1, the clay content of the original tailings (<2 µm fraction) is low, ranging from 0.21 to 4.3% (by weight).

Wiberg et al. (1994) reported that a minimum of 5 to 10% of clay-sized particles (<4 µm) is sufficient to assume control of the erosion process in natural sediments. Soulsby (1970) has also noted that cohesion strongly influences the erosion process if the fine fraction of the sediment (<63 µm) is more than 10%.

Salinity could play a significant role by increasing the critical shear stress (due to flocculation) for surface erosion if it is above 1 g/L (Partheniades 2006). The measured salinity of the site water for the samples studied in the present study were less than 1 g/L, so salinity was deemed to have a negligible effect on the critical shear stress for surface erosion. Therefore, using London tap water instead of the site water in preparing the samples likely did not have significant influence on the magnitude of critical bed shear stress.

### Determination of bed shear stress

The bed shear stress of the tailings and sediments were determined from the near-bed velocity profiles and the change in total pressure in the boundary layer. The velocity field in the annular column was measured with LDV and the change in total pressure in the boundary layer was measured by Preston tube. The details are as follows.

#### Velocity distribution using laser Doppler velocimeter

The water was stirred with the motor driven Teflon stirrer at a speed ranging from 44 to 197 rpm. For each stirrer speed, the vertical velocity profile at radial distances of 14, 11.5, 10, and 7 cm from the centre of the column were measured with LDV. A typical vertical velocity profile at different radial distances from the centre of the column at a stirrer speed of 197 rpm is shown in Fig. 3.

#### Bed shear stress determination from velocity profile

In turbulent flow with smooth bed surface, the viscous shear stress is dominant close to the bottom because the turbulent velocity fluctuations die out near the bottom. Above the viscous sub-layer, the flow is turbulent (van Rijn 1998).

The bed shear stress can be estimated from the velocity profile using eq. [1] provided that the velocity distribution

in the viscous sub-layer follows the law of the wall (eq. [2]). The average bed velocity gradient was calculated using the near-bed velocity data in the viscous sub-layer that showed almost a linear profile.

$$[1] \quad \tau_b = \tau_y + \mu \frac{du}{dz}$$

where  $\tau_b$  is the bed shear stress (Pa),  $\tau_y$  is the yield stress of the suspension in the flow (Pa),  $\mu$  is the dynamic viscosity ( $1.002 \times 10^{-6}$  N·s·m<sup>-2</sup> at 20 °C), and  $du/dz$  is the gradient of the velocity profile near the bed in the viscous sub-layer.

If the concentration of re-suspended tailings and sediments is more than 30 000 mg/L, the flow can be considered as non-Newtonian flow and the flow-induced bed shear stress can be estimated using eq. [1] (accounting for the yield stress due to the water–sediment suspension). In the present study, the concentration of re-suspended tailings in the flow is less than 30 000 mg/L (i.e., the water–sediment suspension shows Newtonian behavior) and so  $\tau_y$  is negligible (Migniot 1968). It should also be noted that  $\tau_y$  is not the yield stress of the bed material; rather it is the yield stress of the suspension.

Equation [1] is used to estimate the bed shear stress on a flat (smooth) bed. However, it is known that once the sediment transport process is established, bed forms will be formed. The existence of these bed forms will introduce additional bed shear stress due to the non-uniform pressure distribution over the bed form crest and eddy region. In the present study, the flow-induced bed shear stress was limited to less than 0.5 Pa by controlling the stirrer speed. The bed shear stress was estimated using eq. [1]. As the flow-induced bed shear stress increases to a larger value, estimating the bed shear stress using eq. [1] will significantly underestimate the actual bed shear stress.

$$[2] \quad U^+ = Z^+ \text{ for } Z^+ \leq 5$$

where  $Z^+ = zu^*/\nu$ ,  $U^+ = u/v^*$ ,  $u^* = \sqrt{\tau_b/\rho}$ ,  $u^*$  is the bed shear velocity (m·s<sup>-1</sup>),  $\tau_b$  is the bed shear stress (Pa),  $\rho$  is the fluid density (kg·m<sup>-3</sup>),  $z$  is the vertical distance from the bottom plate (m),  $u$  is the time average velocity (m·s<sup>-1</sup>), and  $\nu$  is the kinematic viscosity of the fluid (water) in m<sup>2</sup>·s<sup>-1</sup>.

The near bed velocity gradient was computed from the near bed velocity distributions for radial distances of 14, 11.5, 10, and 7 cm from the centre of the column at stirrer speeds of 44, 61, 78, 95, 112, 129, 146, 163, 180, and 197 rpm. Figure 3 presents a typical profile. Using eq. [1], the bed shear stress was computed for the same radial distances and the results are as shown in Fig. 4. Moreover, by averaging the bed shear stress for a given stirrer speed, a linear relationship was established between the average bed shear stress and the stirrer rotational speed (Fig. 4). As a means of validating the estimated (computed) bed shear stress, the velocity distribution in the viscous sub-layer was analyzed using eq. [2] and it is confirmed that it is in line with the law of the wall (typical figure, Figs. 5a–5d).

#### Bed shear stress determination from Preston tube measurement

Preston's method of measuring wall shear stress (skin friction), which makes use of a simple Pitot tube resting on

**Table 1.** Some basic physical properties of the tailings and the sediments.

No.	Description	Unit	Tailings					Sediments				
			Mattabi	Shebandowan-I	Shebandowan (west cell)	Musselwhite	Musselwhite and 5% kaolinite mix	Musselwhite and 15% kaolinite mix	Sudbury	Casco silt	London sand	
1	Specific gravity	—	3.29	3.12	3.30	3.32	3.20	3.25	3.88	2.86	2.76	
2	Gravel size content	%	0.0	0.0	0.0	0.0	0.0	0.0	0.0	0.0	0.0	
3	Fines content (<75 μm)	%	63.6	12.5	59.2	58.00	68.56	77.26	25.47	65.4	1.7	
4	Fines content (<63 μm)	%	45.5	7.6	53.1	51.50	65.44	73.53	21.10	59.2	0.0	
5	Fines content (<5 μm)	%	2.9	0.21	5.1	5.96	10.40	15.89	3.06	9.0	0.0	
6	Clay size particles (<2 μm)	%	2.6	0.21	4.3	2.02	6.52	14.09	1.77	7.5	0.0	
7	D <sub>10</sub>	mm	0.033	0.069	0.017	0.008	0.005	0.004	0.028	0.005	0.122	
8	D <sub>30</sub>	mm	0.073	0.140	0.068	0.026	0.021	0.019	0.075	0.021	0.190	
9	D <sub>60</sub>	mm	0.122	0.216	0.120	0.078	0.044	0.031	0.131	0.074	0.317	
10	D <sub>50</sub>	mm	0.101	0.191	0.097	0.059	0.061	0.050	0.111	0.039	0.255	
11	Plasticity index	%	12.6	—	7.7	4.35	5.5	19.1	4.29	3.1	—	

**Fig. 3.** Vertical velocity profile at different radial distances — for a stirrer speed of 197 rpm using LDV.

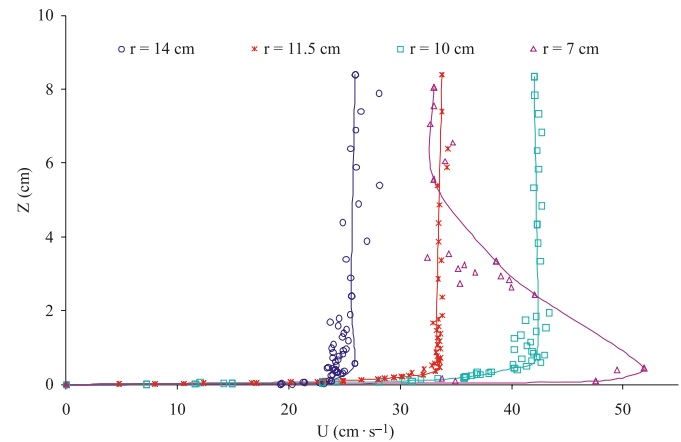
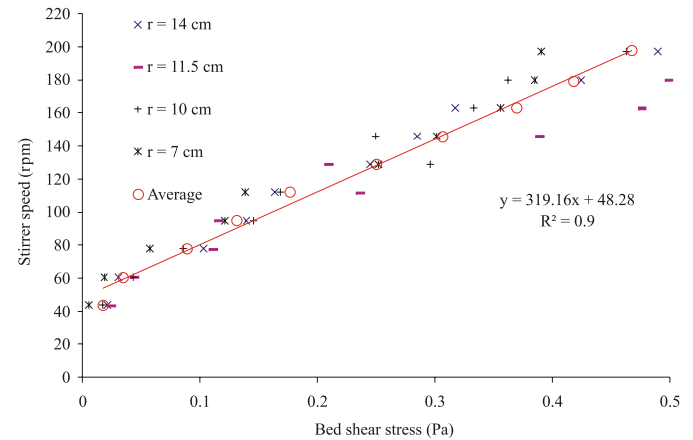


**Fig. 4.** Stirrer speed – bed shear stress relationship using LDV.



the surface (the so-called Preston tube), depends upon the assumption of a universal law of the wall, common to boundary layers and fully developed pipe flow. The non-dimensional relationship between Preston tube reading and wall shear stress can be presented in the form shown in eq. [3] (Patel 1965; Preston 1954).

$$[3] \quad \frac{\tau_b d^2}{4\rho\nu^2} = F\left(\frac{\Delta P d^2}{4\rho\nu^2}\right)$$

where  $\Delta P$  is the Preston tube reading (the difference between total and static pressure) in kPa,  $d$  is the outside diameter of the Preston tube in m,  $\rho$  is the density of the fluid (water) in  $\text{kg}\cdot\text{m}^{-3}$ ,  $\nu$  is the kinematic viscosity of the fluid (water) in  $\text{m}^2\cdot\text{s}^{-1}$ , and  $\tau_b$  is the bed shear stress in kPa.

The widely accepted and the most comprehensive calibration chart by Patel (1965) was used in the present study. As per Patel (1965), the calibration functions are as shown in eqs. [4] to [8].

$$[4] \quad x^* = \log_{10}\left(\frac{\Delta P d^2}{4\rho\nu^2}\right)$$

$$[5] \quad y^* = \frac{1}{2}x^* + 0.037 \text{ for } 0 < x^* < 2.9$$

**Fig. 5.** (a) Validation of the log law in the viscous sub-layer for  $r = 14$  cm, 197 rpm stirrer speed. (b) Validation of the log law in the viscous sub-layer for  $r = 11.5$  cm, 197 rpm stirrer speed. (c) Validation of the log law in the viscous sub-layer for  $r = 10$  cm, 197 rpm stirrer speed. (d) Validation of the log law in the viscous sub-layer for  $r = 7$  cm, 197 rpm stirrer speed.

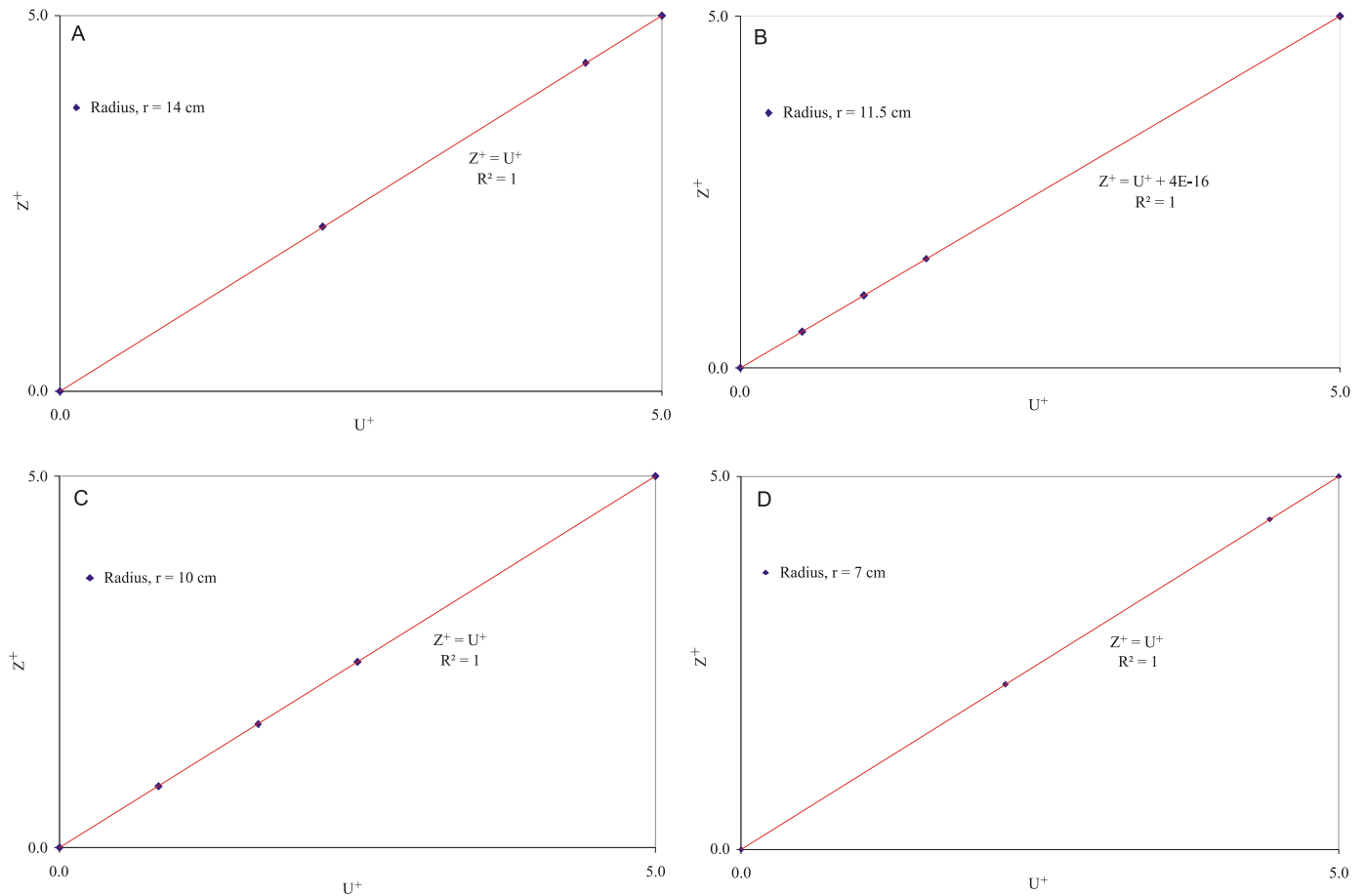
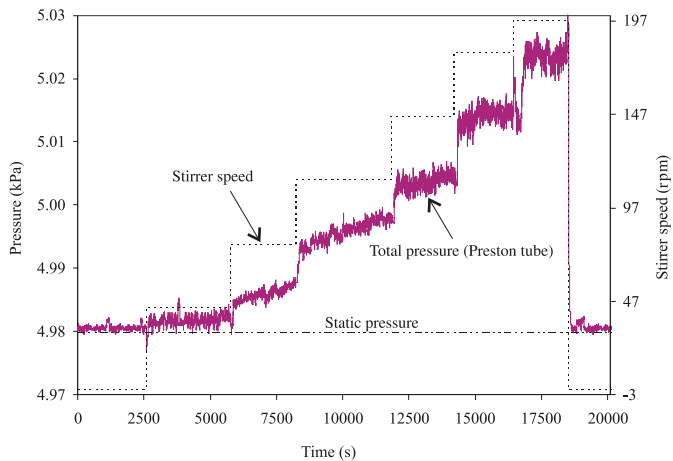


**Fig. 6.** Result of total pressure measured by Preston tube.

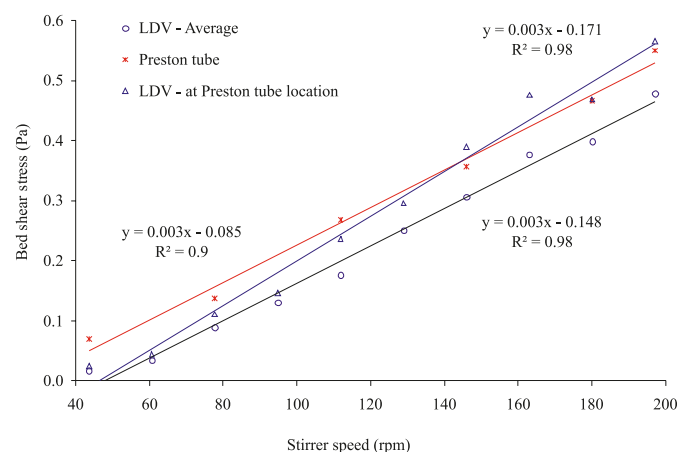


$$[6] \quad y^* = 0.8287 - 0.1381x^* + 0.1437x^{*2} - 0.0060x^{*3} \quad \text{for } 2.9 < x^* < 5.6$$

$$[7] \quad y^* + 2\log_{10}(1.95y^* + 4.10) = x^* \quad \text{for } 5.6 \leq x^* < 7.6$$

$$[8] \quad y^* = \log_{10}\left(\frac{\tau_b d^2}{4\rho v^2}\right) \Rightarrow \tau_b = (10^{y^*})\left(\frac{4\rho v^2}{d^2}\right)$$

**Fig. 7.** Stirrer speed – bed shear stress relationship using LDV and Preston static tube.



The results of the total pressure measured with the Preston tube, and the derived relation between the stirrer speed and bed shear stress are shown in Figs. 6 and 7. The results show that the relation between the near bed shear stress and the stirrer speed is linear ( $R^2 = 0.99$ ).

**Fig. 8.** Time – average concentration and bed shear stress curve for the tailings and sediments.

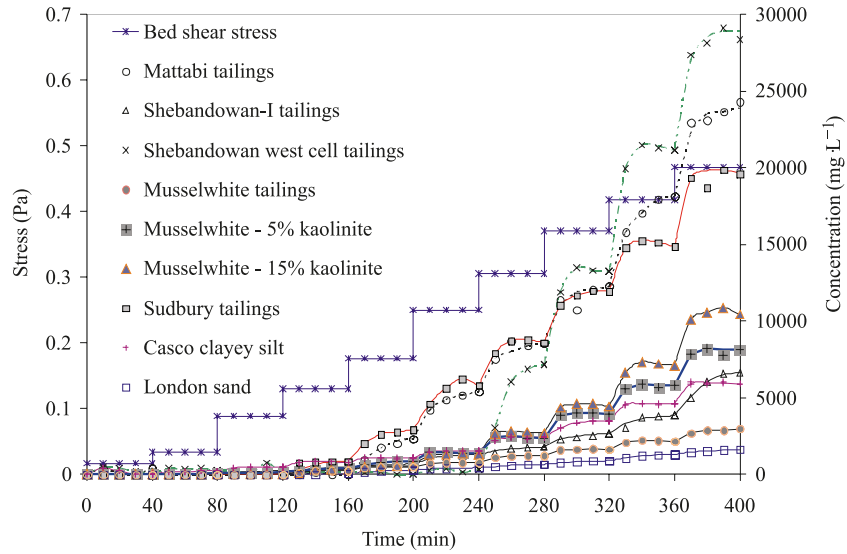


**Fig. 9.** Critical shear stress estimation for the tailings and sediments.

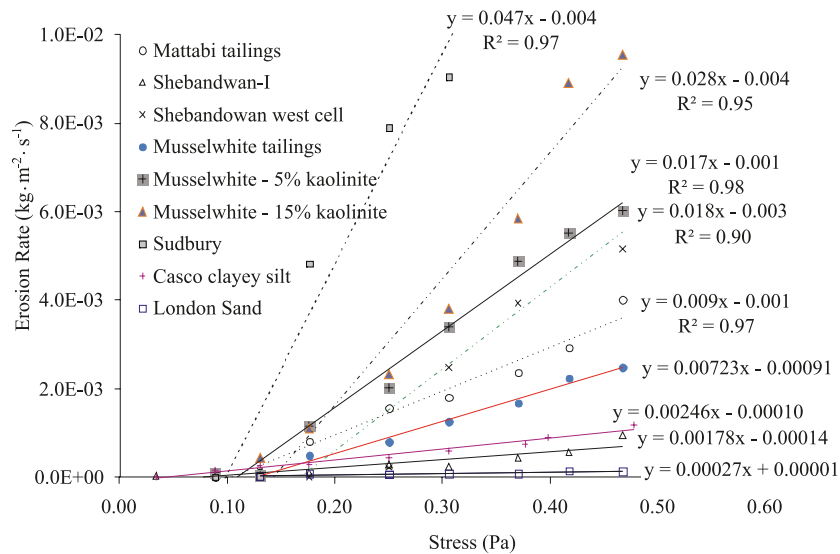


**Table 2.** Critical shear stresses and erosion rates for mine tailings and sediments.

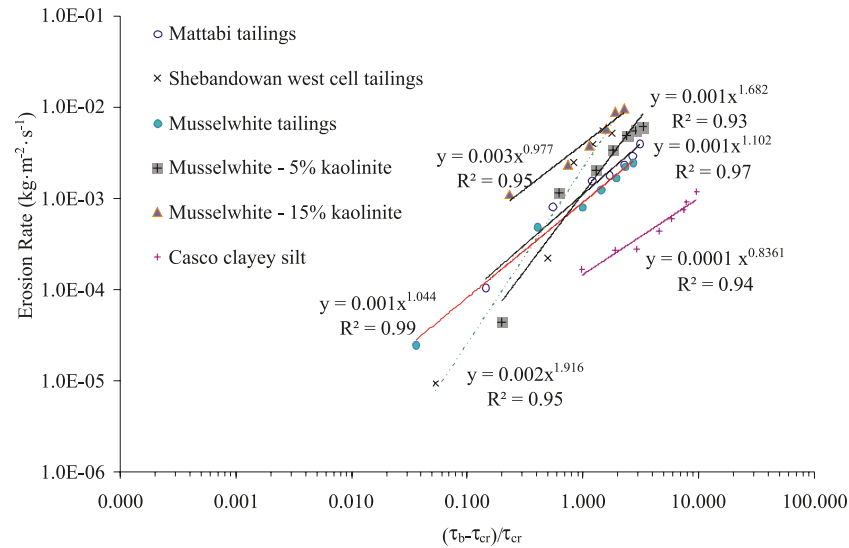
No.	Tailings and sediments	Critical shear stress, $\tau_{cr}$ (Pa)	Erosion rate coefficients		Correlation coefficient, $R^2$
			$\alpha$	$\beta$	
1	Mattabi tailings	0.090–0.114	0.00110	1.10210	0.97
2	Shebandwan-I tailings	0.034–0.078	0.00007	1.11750	0.69
3	Shebandwan west cell tailings	0.130–0.168	0.00210	1.91610	0.95
4	Musselwhite tailings	0.130–0.126	0.00100	1.04400	0.99
5	Musselwhite tailings – 5% kaolinite	0.090–0.109	0.00100	1.10200	0.97
6	Musselwhite tailings – 15% kaolinite	0.090–0.143	0.00300	0.97700	0.95
7	Sudbury tailings	0.090–0.099	0.00100	2.66500	0.79
8	Casco clayey silt	0.017–0.045	0.00010	0.83610	0.94
9	London poorly graded sand	0.090–0.131	0.00002	0.59400	0.56

**Comparison of bed shear stresses from velocity profile and Preston tube**

The bed shear stress was also estimated at the Preston tube location (i.e., at the middle of the annular column) from the velocity profile measured with the LDV. In gen-

eral, the bed shear stress profiles estimated by the two methods are comparable with a difference of less than 10%. Indeed, as shown in Fig. 7, the one measured by the Preston tube was higher than the one estimated from the velocity profile up to a stirrer speed of about 140 rpm and thereafter

**Fig. 10.** Relation between excess shear stress and erosion rate (eq. [10]).



the one estimated from the velocity profile became higher. The Preston tube was placed at the bed surface and had an external diameter of 2.4 mm and should stay in the boundary layer. However, as the stirrer speed gets higher and higher, the thickness of the viscous sub-layer of the turbulent boundary layer gets smaller and smaller. Therefore, after a certain high stirrer speed, the accuracy of the Preston tube will decrease due to the smaller thickness of the boundary layer. Indeed, for surface erosion estimation at low stresses, such as in the present study, the Preston tube is an inexpensive, accurate, and an easy way to measure the bed shear stress.

#### Concentration of re-suspended tailings and sediments

In the present erosion experiments, shear stress was applied (increased) in steps. In each step, the applied shear stress was kept constant for 40 min. This time was fixed by running the erosion test at several single shear stresses and determining the time when the erosion rate went to zero or decreased. In general, the time scale for erosion at a certain shear stress varies between 20 min (Sanford and Maa 2001) and 1 h (HydroQual 2001). These studies have shown that the erosion rate at the beginning of each step was high and decreased with time; it was nearly zero at the end of the steps in most cases (i.e., in 40 min).

As a means of determining the average concentration of re-suspended solids, samples were taken after 10, 20, 30, and 40 min at the beginning of each shear stress increment using the sampling ports. It should be noted that the variation of concentrations taken at different sampling ports on the apparatus were less than 12% from the average concentration. The results of these measurements for Shebandowan-I, Shebandowan west cell, Matabi, Musselwhite, Musselwhite – 5% kaolinite, Musselwhite – 15% kaolinite, and Sudbury tailings, and Casco clayey silt and London sand are as shown in Fig. 8. This figure also shows that the erosion rate was high at the start and nearly nil at the end of each stress step. Indeed, in some of the last shear stress incremental steps, the erosion rate decreased towards the end of the step. This phenomenon is due to the depth rate of change of resistance.

As per Krone (1962), the erosion rate for surface erosion could be estimated using eq. [9]. In the present study, to develop the relation between excess shear stress and erosion rate, the average concentration – time relation was converted to erosion rate using eq. [9].

$$[9] \quad E = \frac{d(hC)}{dt} = \frac{H}{60000} \frac{(C_2 - C_1)}{(t_2 - t_1)}$$

where  $E$  is the erosion rate in  $\text{kg}\cdot\text{m}^{-2}\cdot\text{s}^{-1}$ ,  $H$  ( $= 0.50$  m) is the height of water above the tailings surface in the laboratory column in m,  $C_1$  and  $C_2$  are the average concentrations of re-suspended tailings or sediment particles at the beginning and end of the initial time step (of the shear stress step) in  $\text{mg}\cdot\text{L}^{-1}$ , and  $t_2 - t_1$  ( $= 10$  min) is the initial time step in min.

#### Determination of critical bed shear stress for erosion

For non-cohesive soils, the critical shear stress could be estimated using the Shield's criterion using a representative particle diameter by ignoring the sediments interaction (Shields 1936). For cohesive sediments, the critical shear stress is usually determined experimentally. Indeed, semi-empirical formulas of Dou, Sha, and Tang are usually used to obtain preliminary information on the critical shear stress of newly deposited cohesive sediments (Chien and Zhaohui 1999).

In the present study, the erosion rate for each shear stress step was determined from the measured suspended tailings average concentration – time relationship (Fig. 8). The critical shear stress of the tailings and sediments were determined from the experimentally established relationship between the applied bed shear stress and average concentration of re-suspended solids (Fig. 9). The critical shear stress for erosion ( $\tau_{cr}$ ) of the tailings and sediments were also estimated by visually observing and examining the applied shear stress that actually created “pitting of the surface” and made “the water cloudy”. The visual observations and examinations were done during the erosion experiment by noting the stirrer speed during incipient motion of the particles and estimating the corresponding shear stress from the

developed stirrer speed - bed shear stress relationship (Fig. 4).

The measured critical shear stresses for erosion ( $\tau_{cr}$ ) for the tailings and sediments are as shown in Table 2. The results show that the critical shear stress determined from the relationship between the bed shear stress and average concentrations of re-suspended solids was larger compared to the one determined by visual examination. This is due to the fact that at the time of initiation of motion of re-suspended particles, the concentration is so low that it is difficult to get representative samples with the sampling technique employed in this study.

In general, as shown in Tables 1 and 2, the Musselwhite tailings have a critical shear stress of 0.126 Pa and a plasticity index of 4.35%. When 5% kaolinite clay was added to Musselwhite tailings (Musselwhite – 5% kaolinite mixture), the plasticity index increases to 5.5% while the critical shear stress decreases to 0.109 Pa. When 15% kaolinite clay is added to Musselwhite tailings, the plasticity index and the critical shear stress increase to 19.1% and 0.143 Pa, respectively. This suggests that there is a limiting clay content, depending on the type of clay mineral present in the tailings (i.e., plasticity index) and other influencing factors, for cohesive behavior to develop at the top layer of the deposited tailings. Below this limiting value, the critical shear stress for surface erosion increases gradually and above which the increase is rapid and significant.

#### Effect of clay minerals type on the incipient motion of tailings

Unlike the tailings–kaolinite mixture, attempts to carry out erosion experiments on tailings–bentonite mixture were not successful. A suspension of Musselwhite tailings, bentonite, and London tap water was dispersed and allowed to sit for 8 days to see if it would settle and consolidate, but it did not. This was likely due to the behavior of the sodium bentonite in the suspension. Montmorillonite could be present in mine tailings and if the amount is significant (say, 10% or higher), this could complicate settling and would require the addition of a sufficient quantity of flocculating agents in the mill, prior to disposal of the tailings in the impoundment. This also suggests that flooding of such tailings may not be advisable under prevailing winds.

#### Erosion rate – bed shear stress relationship

The design of an optimum water cover for sulfide bearing tailings is based on a good understanding of tailings erosion. A number of researchers have tried to obtain the relation between erosion rate and excess shear stress of cohesive sediments for different sediments (Krone 1962; Mitchener and Torfs 1996).

The 4 days consolidated samples of the tailings and sediments investigated in the laboratory annular column showed that the finer fractions overlaid the coarser fraction. This was actually due to variations in the settling velocity of the solids and the effect of flocculation. In the first period of the deposition process, solids settle depending on their settling velocities and in the final period due to flocculation effect. Flocculation occurs due to the fact that the smaller particles ( $< \mu\text{m}$ ) in combination with the sufficiently large concentration of the suspension yield relatively small distances be-

tween particles and cause them to collide. Salinity, temperature, and the presence of organic matter influence flocculation (Mitchell and Soga 2005). This causes the critical shear stress for erosion ( $\tau_c$ ) to increase with depth in the bed layer as the sediment density increases with depth. Parchure and Mehta (1985) observed similar depositional effects in cohesive sediments.

During the deposition of Shebandowan-I tailings in the present study, a marked top layer consisting of mud (silt and clay) with a thickness of 3 to 5 mm was observed, while a 3 mm top layer of fine tailings was observed for Mattabi tailings after 4 days of consolidation. A similar effect was observed for the natural sediments. In each case, the rate of surface erosion and re-suspension of the tailings was controlled by the erosion resistance of the top layers. The clay size content of the top layer of the tailings was small and increased significantly due to sorting during deposition. This implies that the cohesion of the whole tailings sample is completely different from the cohesion of the top layer, which actually controls the re-suspension process.

Despite the lack of complete agreement on the appropriate formulation for erosion rate, there is a general agreement that the relationship between the erosion rate and the normalized excess shear stress for a consolidated (or a mechanically emplaced) bed of constant density is given by eq. [10] (Ziegler and Lick 1986; Partheniades 2006).

Based on the measured average concentration of re-suspended tailings and sediments as a function of bed shear stress and time, a relationship between excess shear stress ( $\tau_b - \tau_{cr}$ ) and erosion rate ( $E$ , computed using eq. [9]) was developed for each of the tailings and sediments. The best-fit relation between  $E$  and  $(\tau_b - \tau_{cr})/\tau_{cr}$  for the tailings (Shebandowan west cell, Mattabi, Musselwhite, Musselwhite – 5% kaolinite, and Musselwhite – 15% kaolinite) and Casco clayey silt was found to follow a power law relationship with high coefficient of correlation (Table 2, Fig. 10). However, Shebandowan-I tailings, Sudbury tailings, and London sand did not yield high coefficient of correlation for a power law relationship between  $E$  and  $(\tau_b - \tau_{cr})/\tau_{cr}$  (Table 2). The power law relations obtained from curve-fitting of the tailings and natural sediments erosion data may be described by eq. [10] with the corresponding details as shown in Table 2.

$$[10] \quad E = \alpha \left( \frac{\tau_b - \tau_{cr}}{\tau_{cr}} \right)^\beta$$

#### Summary and conclusions

In the present study, erosion tests were carried out in a Plexiglas annular column on mine tailings and natural sediments. Shear stress was introduced through a motor driven stirrer to investigate initiation of motion and subsequent re-suspension of the mine tailings or sediments. Based on the results, the following conclusions are drawn.

- Unlike an open column, the annular column reduced the accumulation of the tailings or sediments in a particular location by reducing (i.e., re-routing) the vorticity developed by the Teflon stirrer. This, in turn, better channeled the flow and the re-suspended tailings and sediments. A

better channeled flow gives a reliable relation between the average bed shear stress and average re-suspended solids concentration. This, in turn, leads to a better estimate of the critical shear stress ( $\tau_{cr}$ ) and erosion rate coefficients ( $\alpha$  and  $\beta$ ).

- The bed shear stress estimated from the near-bed velocity profile (using LDV) was in a good agreement with values measured with the Preston tube. Therefore, the bed shear stress can be estimated accurately and inexpensively with Preston static tube alone.
- The critical shear stress for erosion ( $\tau_{cr}$ ) for Shebandowan-I, Shebandowan west cell, Mattabi, Musselwhite, Musselwhite – 5% kaolinite, Musselwhite – 15% kaolinite, and Sudbury tailings were in the range 0.034–0.078 Pa, 0.13–0.168 Pa, 0.09–0.114 Pa, 0.0130–0.126 Pa, 0.090–0.109 Pa, 0.090–0.143 Pa, and 0.090–0.126 Pa, respectively. For London sand and Casco clayey silt, the corresponding critical shear stresses were 0.09–0.131 Pa and 0.017–0.045 Pa. The values for the tailings are similar to those reported for natural sediments.
- The best relationship between  $E$  and  $(\tau_b - \tau_{cr})/\tau_{cr}$  for Shebandowan west cell, Mattabi, Musselwhite, Musselwhite – 5% kaolinite, and Musselwhite – 15% kaolinite tailings is a power law with a reasonably high correlation coefficient. However, Shebandowan-I tailings, Sudbury tailings, and London sand did not yield high coefficient of correlation for a power law relationships.
- Montmorillonite could be present in mine tailings and if the amount is significant (say, 10% or higher), this could complicate settling and a sufficient quantity of flocculating agents must be introduced in the mill prior to disposal of tailings in the impoundment.
- It is observed that sorting during deposition plays a prominent role on surface erosion of tailings or sediments. Due to sorting during deposition, the cohesion of the top layer (which controls surface erosion) is different from the cohesion of the whole tailings and sediments.
- For all the mine tailings investigated, with the exception of Shebandowan-I and Sudbury tailings, the developed relation between  $E$  and  $\tau_b - \tau_{cr}$  may be used to estimate the optimum water cover depth. That is, once the wind-induced bed shear stress are estimated, the investigated parameters ( $\alpha$ ,  $\beta$ , and  $\tau_{cr}$ ) may be used to estimate the optimum water cover depth.
- Apart from the percentage of clay and plasticity index, the dominant type of clay mineral present in tailings play a prominent role in the incipient motion of tailings particles in a water cover.

## Acknowledgments

The work described in this paper was supported with funding from Inco Limited and the Natural Sciences and Engineering Research Council of Canada (NSERC) under a Collaboration Research and Development Project Grant awarded to Dr. E.K. Yanful.

## References

Braja, M.D. 2002. Soil mechanics laboratory manual. 6th ed. Oxford University Press, New York.

- Chien, N., and Zhaohui, W. 1999. Mechanics of sediment transport. Translated under the guidance of Jhone S. McNown. American Society of Civil Engineers, Reston, Va.
- HydroQual. 2001. A primer for ECOMSED, Version 1.2, User Manual.
- Krone, R.B. 1962. Flume study of transport in estuarine shoaling processes. Hydraulic Engineering Laboratory, University of California, Berkeley, Berkeley, Calif., USA.
- Mian, M.H., and Yanful, E.K. 2007. Erosion characteristics and re-suspension of sub-aqueous mine tailings. *Journal of Environmental Engineering and Science*, **6**(2): 175–190. doi:10.1139/S06-040.
- Mian, M.H., Yanful, E.K., and Martinuzzi, R. 2007. Measuring the onset of mine tailings erosion. *Canadian Geotechnical Journal*, **44**(4): 473–489. doi:10.1139/T06-116.
- Migniot, C. 1968. Étude des propriétés physiques de différents sédiments très fins et de leur comportement sous des actions hydrodynamiques. *Houille Blanche*, **7**(7): 591–620. doi:10.1051/lhb/1968041.
- Mitchell, J.K., and Soga, K. 2005. Fundamentals of soil behavior. 3rd ed. John Wiley & Sons, Inc., New Jersey.
- Mitchener, H., and Torfs, H. 1996. Erosion of mud/sand mixtures. *Coastal Engineering*, **29**(1-2): 1–25. doi:10.1016/S0378-3839(96)00002-6.
- Parchure, M.T., and Mehta, A.J. 1985. Erosion of soft cohesive sediment deposits. *Journal of Hydraulic Engineering*, **111**(10): 1308–1326. doi:10.1061/(ASCE)0733-9429(1985)111:10(1308).
- Partheniades, E. 2006. Engineering properties and hydraulic behavior of cohesive sediments. CRC Press, Taylor and Francis Group, New York.
- Patel, V.C. 1965. Calibration of Preston tube and limitation on its use in pressure gradients. *Journal of Fluid Mechanics*, **23**(01 I): 185–208. doi:10.1017/S0022112065001301.
- Preston, J.H. 1954. The determination of turbulent skin friction by means of Pitot tubes. *Journal of the Royal Aeronautical Society*, **58**: 109.
- Robertson, J.D., Tremblay, G.A., and Fraser, W.W. 1997. Subaqueous tailings disposal: A sound solution for reactive tailings. In *Proceedings of the Fourth International Conference on Acid Rock Drainage* (Vancouver, British Columbia, Canada), Vol. III. pp. 1027–1041.
- Sanford, L.P., and Maa, J.P.-Y. 2001. A unified erosion formulation for fine sediments. *Marine Geology*, **179**(1-2): 9–23. doi:10.1016/S0025-3227(01)00201-8.
- Shields, A. 1936. Application of similarity principles and turbulence research to bed-load movement. *Mitteilunger der Preussischen Versuchsanstalt für Wasserbau und Schiffbau*, Vol. 26. pp. 5–24. Available from <http://caltechkhr.library.caltech.edu/56/01/Sheilds.pdf>.
- Soulsby, R. 1970. Dynamics of marine sands. A Manual for Practical Applications. Thomas Telford Publishing, London.
- van Rijn, L.C. 1998. The effect of sediment composition on cross-shore bed profiles. 26th ICCE, Copenhagen, Denmark.
- Wiberg, P.L., Drake, D.E., and Cacchione, D.A. 1994. Sediment re-suspension and bed armoring during high bottom stress events on the northern California inner continental shelf: measurements and predictions. *Continental Shelf Research*, **14**(10–11): 1191–1219. doi:10.1016/0278-4343(94)90034-5.
- Ziegler, C.K., and Lick, W. 1988. The transport of fine grained sediments in shallow waters. *Environmental Geology and Water Sciences*, **11**(1): 123–132. doi:10.1007/BF02587771.